

# Ultrasonic signal denoising using hybrid filter for image reconstruction

Shubham Kumar Gupta<sup>1 †</sup>, Azeem Ahmad<sup>2</sup>, Balpreet Singh Ahluwalia<sup>2</sup>, Frank Melandsø<sup>2</sup>, and Anowarul Habib\*<sup>2</sup>

<sup>1</sup>Dept of Chem. Eng., Indian Institute of Technology Guwahati, India

<sup>2</sup>Dept. of Phys. and Tech., UiT The Arctic University of Norway, Tromsø, Norway

## 1. Introduction

Lead zirconate titanate (PZT) is an inorganic compound with the chemical formula  $\text{Pb} [\text{Zr}_x \text{Ti}_{1-x}] \text{O}_3$ . It is a perovskite ceramic material with a strong piezoelectric effect, meaning that the compound changes shape when an electric field is applied. Ultrasound transducers, sensors and actuators, high-value ceramic capacitors, etc. are all made of this piezoelectric material<sup>1</sup>). When exposed to extremely harsh environmental conditions, this material can develop a variety of surface and subsurface defects. Due to the concentration of operational stress on these defects, they impair the material's durability, functionality, and, ultimately, performance. As a result, it is crucial to detect and eliminate any defects in the PZT material to ensure proper operation. Here, a technique named dual point excitation and detection was used, as it has the primary advantage of enabling wideband excitation and detection. While the generated images contain a high level of noise, particularly at the subsurface, so it is difficult to gain a precise understanding of the properties of the defects present in the material without first removing the noise from the images. As a result, Here hybrid filter was designed to remove this noise. Denoising an image can be accomplished in a variety of ways<sup>2-4</sup>). Denoising methods can be broadly classified into spatial domain methods and transform domain methods. Spatial filters which are further categorized into linear and non-linear filters utilizes low pass filtering on image pixel values as the noise tends to occupy higher regions in the frequency spectrum. After examining the noise model in the images, a systematic hybrid denoising method was proposed to achieve optimal results for studying these defects in the PZT material. The main aim of this paper is to demonstrate how our hybrid filter can be used to denoise images generated by the dual point excitation and detection method for detecting surface damage in the PZT ceramic disc.

e-mail: anowarul.habib@uit.no

## 2. Experiments, results, and discussions

Our group has previously provided a comprehensive overview of the excitation and detection probes fabrication, as well as the experimental setup<sup>5-9</sup>). This experimental technique for point contact excitation and detection is based on Coulomb coupling technique. It is designed for the excitation and detection of ultrasonic waves in a piezoceramic. A  $20 \times 20 \text{ mm}^2$  PZT with a thickness of 3 mm was used, and a surface damage was introduced.

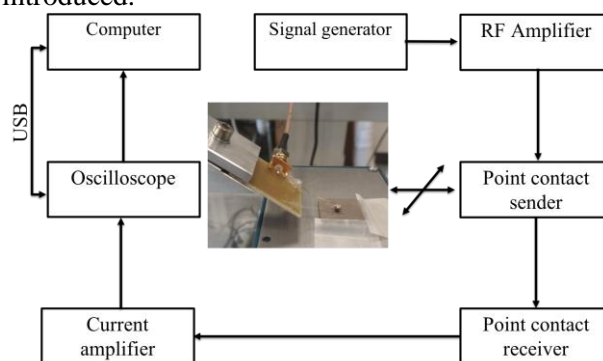
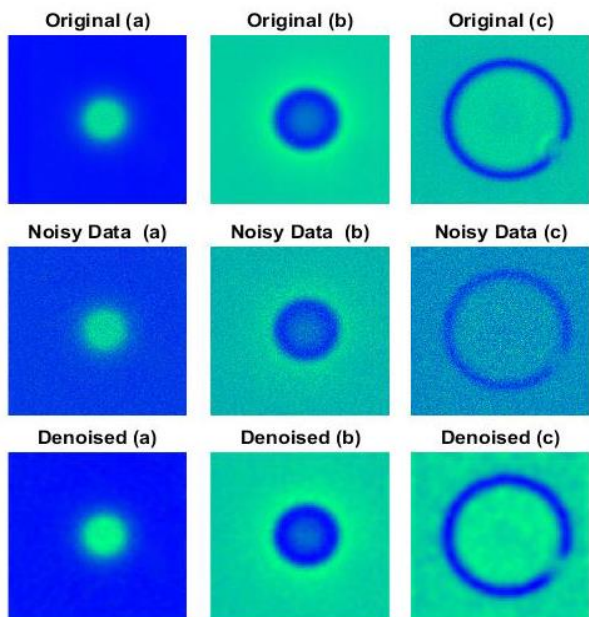


**Fig. 1:** Point contact excitation and detection method

Fig. 1 depicts the experimental setup schematically. To excite the ultrasonic signal in PZT, a Dirac delta pulse with a width of 60 ns was used. The step size was set to  $50 \mu\text{m}$  in both the x and y directions. A default noise adding option from oscilloscope (Agilent 3024A) was employed for adding noise in the excitation signal. The objective of the experiment was to visualize the wave propagation in the PZT sample and localize the defect in the sample.

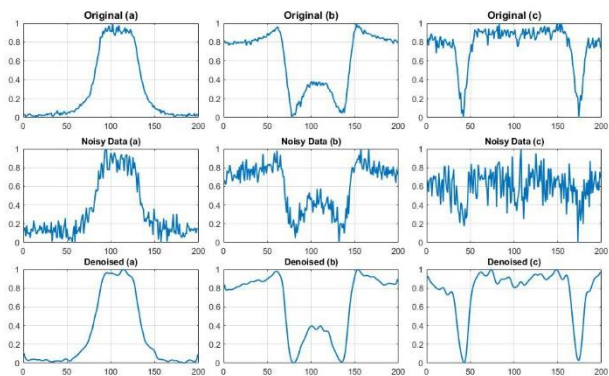
Hybrid filter works with adaptive and non-adaptive filtering to denoise these types of noisy images. Filtering required the use of a single frame for each pixel, composed of neighboring pixels of a specified size, to estimate and produce image deviations.

Fig. 2 illustrates images that have been denoised using proposed hybrid filter.



**Fig. 2:** Ultrasonic wave images in three different time frames, original, noisy data and denoised data. Each frame contains a  $10 \times 10 \text{ mm}^2$  image

To measure the accuracy, the noise-free reference image existing which can be compared finally. It was visually observed that denoising process by plotting the pixel intensities along a horizontal line passing through the center of both the original and denoised images, as illustrated in Fig. 3.



**Fig. 3:** Values of intensity along a common line in images of three distinct time periods

After calculating the Peak Signal-to-Noise Ratio (PSNR) and Structural Similarity Index (SSIM) values, then energy of the noise removed from the original image was calculated. The MSE (Mean Squared Error) and PSNR are used to evaluate the quality of image compression. The MSE calculates the difference in peak error between the compressed and original images, whereas the PSNR calculates the difference in peak error. The MSE value is directly proportional to the error. To calculate PSNR, the block first calculates MSE using the following equation.

$$MSE = \frac{1}{m \cdot n} \sum_{i=0}^{m-1} \sum_{j=0}^{n-1} [I(i,j) - K(i,j)]^2$$

Here, m and n are the input image rows and columns in the previous equation. The PSNR is then calculated as follows:

$$PSNR = 10 \log_{10} \left( \frac{R^2}{MSE} \right)$$

Here, R is the maximum possible pixel value of the image.

**Table 1:** PSNR and SSIM value of denoised image compared to clean image

	Image (a)	Image (b)	Image (c)
PSNR	71.604	69.800	66.624
SSIM	0.9993	0.9990	0.9979

### 3. Conclusion

The acoustic waves in PZT ceramics are excited using a 60 ns delta pulse. A hybrid filter was used to effectively investigate the surface defects in a PZT ceramic and the denoising systems derived from its images, and a previously unknown metric for quantifying noise was proposed. Finally, the reference data is used to determine the PSNR and SSIM values.

### Acknowledgement

Authors acknowledge the funding from Research Council of Norway, INTPART project (309802).

### References

- 1) A. Aabid, B. Parveez, M.A. Raheman, Y.E. Ibrahim, A. Anjum, M. Hrairi, N. Parveen and J. Mohammed Zayan: *Actuators*, 2021,101.
- 2) L. Fan, F. Zhang, H. Fan and C. Zhang: *Visual Computing for Industry, Biomedicine, and Art*. **2** (2019)1.
- 3) D.T. Kuan, A.A. Sawchuk, T.C. Strand and P. Chavel: *IEEE Trans. Pattern Anal. Mach. Intell.* (1985)165.
- 4) J. Portilla, V. Strela, M.J. Wainwright and E.P. Simoncelli: *IEEE Trans. Image Process.* **12** (2003)1338.
- 5) V. Agarwal, A. Shelke, B. S. Ahluwalia, F. Melandsø, T. Kundu and A. Habib: *Ultrasonics*. (2019).
- 6) A. Habib, E. Twerdowski, M. von Buttlar, M. Pluta, M. Schmachtl, R. Wannemacher and W. Grill: *Proc. of SPIE*, 2006, 61771A.
- 7) A. Habib, E. Twerdowski, M. von Buttlar, R. Wannemacher and W. Grill: *Proc. of SPIE*, 2007, 653214.
- 8) A. Habib, A. Shelke, M. Pluta, U. Pietsch, T. Kundu and W. Grill: *AIP Conf. Proc.*, 2012, p. 247.
- 9) A. Shelke, A. Habib, U. Amjad, M. Pluta, T. Kundu, U. Pietsch and W. Grill: *Proc. of SPIE*, 2011, 798415.